A highly efficient 2D flood model with sub-element topography

[1] **Sam R. Jamieson** MSci
PhD Candidate, Heriot-Watt University, Edinburgh in partnership with HR Wallingford, Wallingford, UK

[2] **Julien Lhomme** MSc, PhD
Senior Scientist, HR Wallingford, Wallingford, UK

[3] **Grant Wright** MEng, PhD
Lecturer, Heriot-Watt University, Edinburgh, UK

[4] **Ben Gouldby** BSc
Principal Scientist, HR Wallingford, UK and IH Cantabria, Spain

The need for large- (region-)scale probabilistic simulations means that 2D inundation models are still limited by computational requirements. In addition to parallelisation and physical process simplification, attempts to reduce runtimes typically involve coarsening the computational mesh, which can smooth important topographic features and hence limit accuracy. This paper presents a new 2D flow model that uses an enhanced diffusion-wave, and incorporates sub-element topography in a computational mesh that adapts to the terrain features. The model utilises a fine topographic resolution without having to use a fine computation mesh, and so achieves fast computational runtimes. The model has been tested against the Environment Agency's 2D benchmarking tests, and even though the model is designed to operate at larger spatial scales than those in the benchmarking tests, it is shown to provide comparable accuracy relative to a selection of conventional 2D models, at significantly faster computational speeds. The model therefore has the potential to offer a step change in performance of large-scale probabilistic flood mapping and systems flood risk analysis modelling.

Notation

A_i	impact zone plan area (m²)
A_p	panel flow area (m²)
c	celerity of a wave (m/s)
f	an interface between impact zones
g	gravitational acceleration (m/s²)
h_i	impact zone water depth (m)
i, j	impact zones
n	Manning's coefficient of friction
$\boldsymbol{n}_j$	directional unit vector between an impact zone and its neighbour j
P_p	panel wetted perimeter (m)
p	interface panels/sections
Q_f	interface flow rate (m³/s)
Q_p	panel flow rate (m³/s)
R_p	panel hydraulic radius (m)
S_f	interface water surface slope (m/m)
t	time (s)
$\boldsymbol{u}_i$	impact zone velocity vector (m/s)
V_i	impact zone volume (m³)
w_f	interface width (m)
X_i	impact zone cross-sectional flow area (m²)
η_f	interface water level (m)
η_i	impact zone water level (m)
α	constant used for scaling the Courant number
β	constant used for velocity calculation
ς_p	frictional wetted height on panel sides (m)
Δx	sub-element (or panel) cell width (m)

1. Introduction

Large-scale flood mapping is a primary requirement of the Floods Directive (EC, 2007), and probabilistic flood risk models that require computationally efficient 2D components are in increasing demand. The Environment Agency of England and Wales' (EA) national flood risk assessment (NaFRA) (Environment Agency, 2009) and modelling decision support framework (MDSF2) (Environment Agency, 2011) have utilised simplified inundation models for almost a decade, due to the number of simulations required to undertake comprehensive risk analyses (Gouldby et al., 2008a; Hall et al., 2003). These risk models have also been successfully applied for a wide range of other purposes (e.g. Evans et al., 2006; Gouldby et al., 2008b; Woodward et al., 2011), and there is increasing demand to improve the reliability of the results, particularly the inundation aspects (National Audit Office, 2011).

Water Management
Volume 165 Issue WM1

**A highly efficient 2D flood model with
sub-element topography**
Jamieson, Lhomme, Wright and Gouldby

It is well established that for a given hydrological input, ground elevation and topographic features dominate the hydraulic inundation process (Romanowicz and Beven, 2003; Zhang and Cundy, 1989). In small-scale studies, particularly urban environments, computational grid sizes must be of the order of $1-5$ m to appropriately characterise the underlying topography (Mark *et al.*, 2004). In practice, however, large-scale and probabilistic simulations can rarely be completed at this resolution. Reducing the grid size, for example, has a dramatic effect on the computational cost associated with full shallow-water equation (SWE) models and, counterintuitively, regular grid diffusion-wave models tend to be even slower at such resolutions (Hunter *et al.*, 2008).

While it is evident that 2D inundation simulations over large areas cannot be achieved with grids of equivalent length-scale to natural topographic variation, using traditional grids with coarse resolution can artificially smooth important topographic features. To address this shortcoming, there has been increasing development of models that employ a sub-grid representation with the aim of improving topographic detail while maintaining computational efficiency (Casulli and Stelling, 2011; Hartnack *et al.*, 2009; McMillan and Brasington, 2007; Yu and Lane, 2006b). Yu and Lane (2011) found that post-processing of the DEM to re-introduce the topographic features improves the simulation accuracy of their sub-grid approach. This demonstrates that although accounting for sub-grid mass storage effects, most sub-grid approaches have difficulty representing sub-grid flow blockage effects unless the grid cell boundaries are perfectly aligned with topographic features. An exception to this is the multi-layered approach of Chen *et al.* (2008), which can cope with urban flow blockages within a grid cell. Yet this is limited to simplistic building layouts and it would be difficult to apply to real catchment topography. For coarse modelling this issue was avoided in the past by using manual delineation of flood cells along floodplain features, such as railway embankments and dykes (Estrela and Quintas, 1994; Romanowicz *et al.*, 1996; Zanobetti *et al.*, 1970), but manually creating such grids is subjective and expensive and cannot be practically undertaken at a large scale.

This grid issue has, to some extent, been resolved by the rapid flood spreading method (RFSM) (Gouldby *et al.*, 2008a; HR Wallingford, 2006), wherein computational elements, known as impact zones, are automatically defined to precisely follow topographic features. In addition, the sub-element topography is resolved at the level of the underlying digital elevation model, and so always captures the critical topographic crests causing flow blockage, without the need to manually re-introduce these features.

The RFSM was first implemented with a simple spreading algorithm that conserved volume but did not represent the temporal evolution of the flood wave (direct RFSM). This was later improved with a version that attempted to account for the frictional and dynamic effects of floodplain propagation, using a simplified approach (Lhomme *et al.*, 2009). More recently, attempts have been made to improve process representation by incorporating a time-stepping analytical approximation to the diffusion wave (dynamic RFSM) that is similar in dynamics to the raster storage model Lisflood-FP (Bates and De Roo, 2000). Output from this model compared well with that from a full SWE model on a large-scale site in Ireland (Lhomme *et al.*, 2012), but less well when employed in the EA's 2D hydraulic modelling benchmark tests (Wright *et al.*, 2012). Under these tests, accuracy was constrained due to the use of a constant time step and flow limiters, as has been demonstrated in other diffusive-type models (Hunter *et al.*, 2005).

This paper presents a new version of the RFSM model that overcomes some of the limitations noted above. This new model, RFSM-EDA (RFSM – explicit diffusion wave with acceleration term) – follows the sub-element impact zone approach but uses a new formulation, similar to the diffusion wave but incorporating the local acceleration term of the Saint Venant equations (Bates *et al.*, 2010). An adaptive time step has been implemented, and all flow limiters have been removed. The effectiveness of the model is demonstrated using a selection of the EA's 2D hydraulic benchmark tests (Wright *et al.*, 2012).

2. Model

RFSM-EDA is based on the same mesh concept as the direct RFSM (Gouldby *et al.*, 2008a; Lhomme *et al.*, 2009) and the dynamic RFSM (Environment Agency, 2010, Lhomme *et al.*, 2012). See Figure 1 for a mesh schematic. It incorporates the following primary assumptions.

- The domain can be divided up into discrete and hydraulically consistent topographic depressions, called impact zones (IZs).
- The water surface elevation within each IZ is constant.
- The relationship between water surface elevation and volume in an IZ can be defined by a non-hysteretic relationship.
- The flow rates between neighbouring IZs are calculated linearly across the interface between them, independently of other neighbours.
- The interface can be characterised by a level–width relationship, where the width is assumed to increase with increasing level.

2.1 Pre-processing algorithm

Before computation can begin, the IZs are defined through a pre-processing algorithm. In a first stage, IZs are delineated around collections of cells which, following the line of greatest slope, would drain to the same topographic low point. This produces IZ boundaries defined along topographic crests and high points. In a second stage, the original IZs are modified to ensure that they are above a certain minimum area, and that the interfaces between them are above a minimum communication depth. These modifications are controlled by user-defined parameters; appropriate values will vary depending on the landscape and the DEM resolution. Finally, the level–volume and neighbour level–width
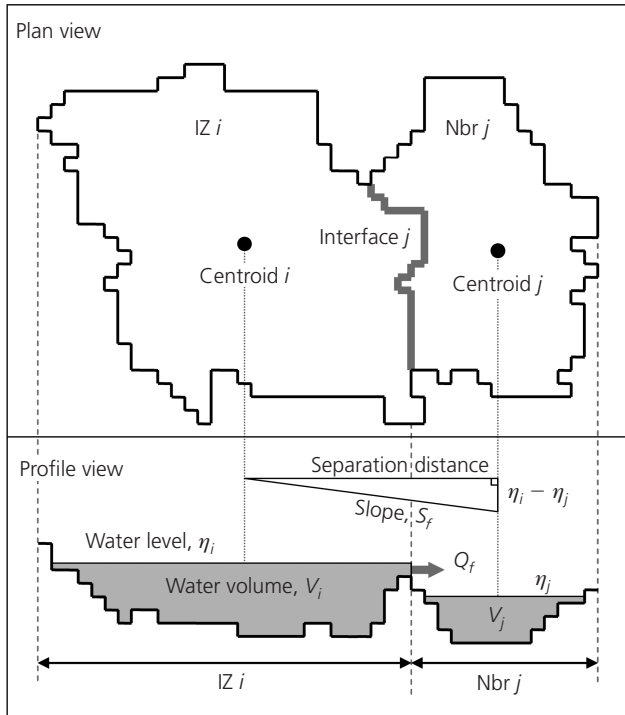
Figure 1. Schematic of an impact zone with a neighbour, in plan and profile. Showing irregular boundaries and selected key variables. Solid grey represents a volume of water

relationships are calculated, and the results are written to a database.

2.2 Governing equations

The derivation of the flow equations stems from the approach of Bates *et al.* (2010). Starting with the one-dimensional Saint Venant equations, advection is assumed negligible and the equations are discretised semi-implicitly, but rearranged into an explicit form. The hydraulic radius is calculated in full including the friction on the side of cells. This differs from other models (e.g. Bates *et al.*, 2010; McMillan and Brasington, 2007; Yu and Lane, 2006a) because the assumption that friction is only encountered on the cell base may not be appropriate in highly variable terrain. A single flow is required for each neighbour interface, *f*, but to avoid sudden changes in hydraulic radius in complex topography, the fluxes are evaluated as the sum of individual fluxes across a number of interface panels, equal to the number of sub-element cells, *p*, in the interface:

$$1. \quad Q_f^{t+\Delta t} = \sum_p \frac{(Q_p^t - g\Delta t A_p^t S_f^t)}{1 + g\Delta t n^2 |Q_p^t|/A_p^t (R_p^t)^{4/3}}$$

where Q_f is the interface flow, Q_p is the panel flow, t is time, g is gravitational acceleration, A_p is panel area, R_p is hydraulic radius of the panel, n is Manning's coefficient and S_f is the water

surface slope across the interface. See Figures 1 and 2 for schematic diagrams showing the relationship between the variables.

The panel hydraulic radius is calculated by

$$2. \quad R_p^t = \frac{A_p^t}{P_p^t}$$

The panel area, A_p, is the difference between the interface water level, η_f, and the panel ground level, z_p, multiplied by the sub-element cell width, Δx:

$$3. \quad A_p^t = \Delta x(\eta_f^t - z_p)$$

The panel wetted perimeter, P_p, is the summation of the wetted base (i.e. the width of the sub-element cell) and the wetted height to one or both of the adjacent panels, ς_p:

$$4. \quad P_p^t = \varsigma_p + \Delta x$$

To evaluate A_p, the interface flow level, η_f, is needed, and a number of different approaches can be applied. Using the mean of the levels in the adjacent IZs is problematic because negative depths occur when the downstream level is below the interface crest. The dynamic RFSM (Lhomme *et al.*, 2012) avoids this by switching to the upstream level when the mean level would create a negative depth. However, this can cause sudden and cyclical jumps in the interface depth if the downstream level fluctuates
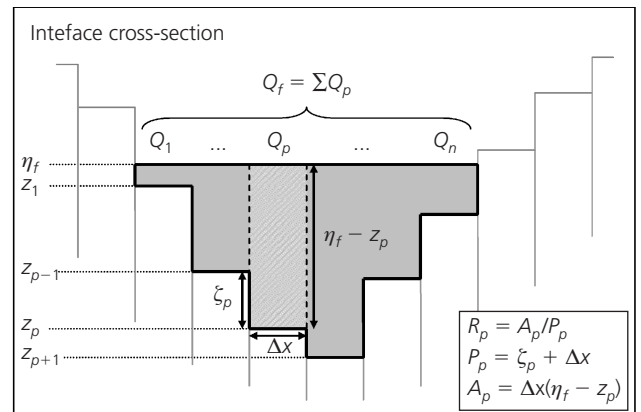
Figure 2. Schematic of an interface between two neighbouring impact zones. Solid grey colouring represents water part-submerging the interface, and the demarked rectangle represents a calculation panel corresponding with an individual sub-element cell

around the level of the interface. In RFSM-EDA a smoother result is obtained by always using the upstream level:

5. $\quad \eta_f^t = \max(\eta_i^t, \eta_j^t)$

The interface slope, S_f, is calculated by dividing the difference in neighbouring IZ water levels by the separation distance between their centroids.

The solution is progressed by applying the conservation of mass:

6. $\quad V_i^{t+\Delta t} = V_i^t + \Delta t \sum_j Q_f^{t+\Delta t}$

where V_i is the volume in IZ i, and j is an IZ neighbour of i. V_i is a function of η_i, the IZ water level, and this relationship is defined in advance in look-up tables created during the pre-processing stage. Therefore, the IZ volume can be efficiently converted into a water level for use in the flux calculations.

2.3 Numerical stability
The scheme is subject to the Courant–Freidrichs–Lewy (CFL) condition, which is satisfied by ensuring that the domain of dependence of the interfaces of an IZ should not exceed the area of the IZ, as used by Guinot and Soares-Frazao (2006). This version of the CFL condition is more appropriate for irregular-shaped elements than that used by Bates *et al.* (2010), because it uses areas rather than lengths. It also differs by including velocity with celerity. The maximum permissible time step, Δt_{max}, is given by

7. $\quad \Delta t_{max} = \alpha \min \dfrac{A_i^t}{\sum\limits_j w_f \max \left(\|\boldsymbol{u}_i^t\| + c_i^t, \|\boldsymbol{u}_j^t\| + c_j^t \right)}$

where α is a constant used to scale the predicted time step, A_i is the surface area of i, w_f is the interface width, $\boldsymbol{u}_i$ is the magnitude of the IZ velocity vector, and the celerity of a wave, c, is given by

8. $\quad c_i^t = \sqrt{gh_i^t}$

where h_i is the depth of water in IZ i.

2.4 Wetting/drying
In some reduced complexity models an algorithm is used to reduce over-rapid wetting or drying (Bradbrook *et al.*, 2004; Yu and Lane, 2006a). As the IZs are assumed to have topographic barriers as crests between them, when an IZ initially wets, the water cannot leave until it fills the volume below the lowest

interface level of its neighbours. Similarly, as an IZ dries, inappropriately large flows will not cause a negative depth, as the stored volume below the minimum interface level will absorb the excess flux. These effects, resulting from the IZ shape, provide a natural resistance to model instability. Therefore no special wetting or drying treatments are explicitly represented within the model.

2.5 Velocities
The velocities calculated at the interfaces could be used as a surrogate for the IZ average velocity in flat topography, but this is not appropriate when the IZs have a depression-like shape. In this case the interface velocities are expected to be relatively shallow and fast, compared with deeper and slower flow conditions at the IZ centre. To convert the interface velocities to an area-average velocity vector, an additional step is necessary. Assuming the IZs are of regular shape, the volume of water that has been fluxed out of the IZ (using the results of Equation 1) is divided by the area of a representative cross-section through the centre of the IZ, X_i:

9. $\quad \boldsymbol{u}_i^t = \dfrac{\Delta t \sum\limits_j Q_j^t \boldsymbol{n}_j}{X_i^t} \qquad$ where $\quad Q_j^t > 0$

where $\boldsymbol{n}_j$ is the unit vector between the IZ and neighbour centroids, used to provide the velocity as a vector. Whether the IZ shape is assumed cubic, cylindrical or as an inverted cone, the calculation for the IZ cross-sectional area can be written as

10. $\quad X_i^t = \beta \sqrt{(h_i^t V_i^t)}$

where β is a constant which for the aforementioned shapes takes on a value between 0·96 and 1·13. As we assume the IZs to be of variable shapes and sizes, β is given a value of 1 for simplicity. It is important to note that this velocity does not impact on the fluxes between IZs, which are calculated independently. The only impact it has on the model is through the CFL condition (Equation 7).

3. Application

3.1 ▪▪▪▪▪▪

3.1.1 Environment Agency benchmark tests
The EA has produced a set of hydraulic benchmark tests designed to test a range of predictive abilities of 2D inundation models. Details of the test specifications are provided in Wright *et al.* (2012) and Environment Agency (2010), so they are only briefly described in this paper. RFSM-EDA has been assessed on most of these tests, although only the results of tests 2A, 4, 5 and 8A are shown here. Table 1 provides a breakdown of the tests, with a justification provided for those not shown.

Water Management
Volume 165 Issue WM1

A highly efficient 2D flood model with
sub-element topography
Jamieson, Lhomme, Wright and Gouldby

Test	Shown in paper?	Reason
1	✗	RFSM-EDA, as most models, performs well on this test, but there is little of interest in the results
2A	✓	See Section 3·2
3	✗	A test of momentum conservation, which the numerical scheme of RFSM-EDA is not expected to achieve
4	✓	See Section 3·3
5	✓	See Section 3·4
6	✗	Dam break scenarios require a full SWE scheme with shock-capturing ability, so RFSM-EDA is not tested
7	✗	Dynamic linking with a 1D element has not yet been tested for RFSM-EDA
8A	✓	See Section 3·5
8B	✗	Dynamic linking with a 1D element has not yet been tested for RFSM-EDA

Table 1. Benchmarking tests that have been completed, and
justification for those not

3.1.2 Comparison with other models

RFSM-EDA has been compared against a number of other models to provide a context for the results, rather than to draw specific conclusions about these individual models. While this is not a rigorous test of the model's validity, in the absence of validation data the model is compared with a range of respected and widely used models. Two finite-volume SWE models are shown, InfoWorks-ICM (Innovyze, 2011; Lhomme *et al.*, 2010) and Tuflow-FV (2nd-order spatial accuracy) (Environment Agency, 2010). Three simplified models are also shown: JFLOW-GPU, a regular grid diffusion-wave model (Bradbrook *et al.*, 2004; Lamb *et al.*, 2009); the dynamic RFSM, also a diffusion-wave model but with the same sub-element representation as RFSM-EDA (Environment Agency, 2010; Lhomme *et al.*, 2012); and Lisflood-ACC, which has a similar numerical approach to RFSM-EDA but is based on a regular grid (Bates *et al.*, 2010; Neal *et al.*, 2011). For these tests all the models adhered to the test specifications apart from the dynamic RFSM, which used an equivalent (though not identical) mesh to 'mesh A' used by RFSM-EDA, described in the following section.

3.1.3 Application of RFSM-EDA

The primary results for RFSM-EDA are created using a mesh significantly coarser than in the other models, but with a sub-element cell resolution corresponding to the specified grid resolution of the tests. This is called mesh A. However, some extra simulations have been carried out using different computational meshes that offer additional insight. Mesh B uses a similarly coarse computational grid, but utilises the finest topographic resolution available in the raw DTM for its sub-element resolution. Mesh C replicates the test specification exactly, like the other models. This means using a fine computational mesh, with each RFSM-EDA mesh element containing one topographic sub-element cell. A summary of the three mesh types for the different tests is provided in Table 2.

For meshes A and B, the results have been produced with

significantly coarser meshes than recommended, and this should be noted when considering the results. For example, the comparative models have extracted results from small grid cells containing only the specified test points, whereas RFSM-EDA uses considerably larger computational elements, which may represent the hydraulic conditions not just in the location of the test points but at distal locations as well.

Mesh C has been used for tests 2A and 5 for comparative purposes, but in practice RFSM-EDA would not be used on such a mesh, as there are no benefits in using the IZ methodology when each IZ contains only one sub-element cell. In fact, the additional computational overhead of the sub-element approach (e.g. calling volume/level look-up tables) makes the use of IZs with one sub-element cell, or only a few cells, more costly than using 'traditional' grids.

All the RFSM-EDA simulations were completed on a machine running Windows XP with a 3·0 GHz processor and 8 GB of RAM, connecting to an SQL database on a network server.

3.2 Test 2: Filling of floodplain depressions

Test 2 is designed to demonstrate a model's ability to deal with inundation processes in a low-momentum event. The test is a square domain of 16 topographic depressions, with test points in each, and an inflow hydrograph in the top left corner. This is an extreme test of the IZ schematisation; rather than the specified ~10 000 elements, the RFSM-EDA mesh A uses only 16 automatically generated elements, one per depression. This means that mesh A had 625 times fewer computational elements, with the same 20 m topographic resolution. RFSM-EDA is capable of further increasing the topographic resolution, and mesh B has the same 16 elements, but with a 2 m topographic resolution, 10 times greater than the other models. Mesh C has the recommended 10 000 elements. See Table 2 for details.

Figure 3 shows the model results at test point 4 (closest to the

EA Test	Test specification	Details of RFSM-EDA meshes					
		Mesh A		Mesh B		Mesh C	
	Cell size: m² (~no. of elements)	Average IZ size: m² (no. of IZs)	Sub-element cell size:m²	Average IZ size: m² (no. of IZs)	Sub-element cell size: m²	Average IZ size: m² (no. of IZs)	Sub-element cell size: m²
2A	400 m² (10 000)	250 000 m² (16)	400 m²	250 000 m² (16)	4 m²	400 m² (10 000)	400 m²
4	25 m² (80 000)	2 300 m² (861)	25 m²	Not undertaken		Not undertaken	
5	2 500 m² (7 600)	35 000 m² (530)	2 500 m²	Not undertaken		2 500 m² (7 643)	2 500 m²
8A	4 m² (97 000)	212 m² (1 786)	4 m²	174 m² (2 207)	0·25 m²	Not undertaken	

Table 2. Details of mesh sizes and sub-element cell resolutions for meshes A, B & C.
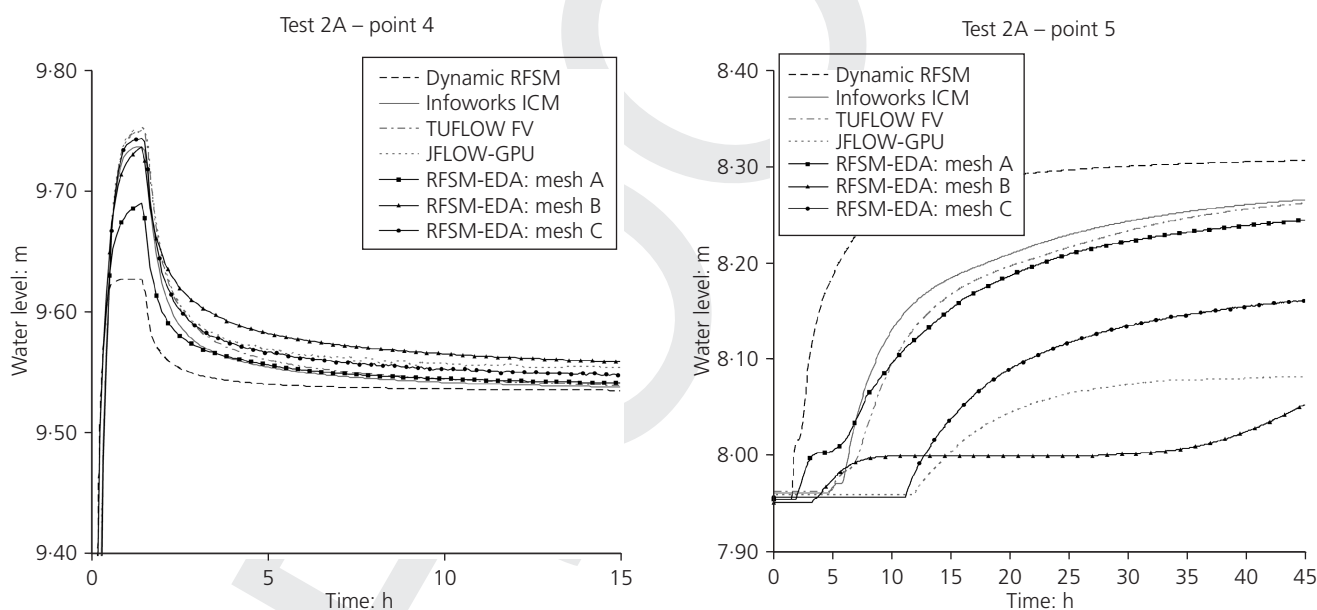
Figure 3. Level plots for test 2 – points 4 and 5

boundary condition) and point 5 (the farthest point from the boundary condition, which receives a significant flow of water). At point 4, RFSM-EDA's mesh A results have a similar profile to the other models, but the peak level is ~4−6 cm lower. The final level matches the other models exactly. At point 5 there is a large spread in the results of all models, not just the ones shown here (Environment Agency, 2010). Even so, RFSM-EDA's results closely match those of Tuflow and InfoWorks, and from 6 h on they remain within 2 cm of Tuflow. RFSM-EDA predicts the water levels to rise ~2·5 h earlier than the other models. This is

due to the large IZs of RFSM-EDA. When water over-tops the preceding crest it immediately fills up from the IZ base (the location of the test point). For the other models the water must travel through a number of cells after the crest before it reaches the test location.

Mesh B produces a response that is quite different from the other models (Figure 3). Although it matches the peak level of the other models at point 4, the final level is 1−2 cm higher. This is because, rather than averaging the DEM to 20 m, it utilises all

Water Management
Volume 165 Issue WM1

**A highly efficient 2D flood model with
sub-element topography**
Jamieson, Lhomme, Wright and Gouldby

the topographic information available at a 2 m resolution. There-fore, this mesh depicts the crests with a higher level of accuracy than the models using the averaged 20 m DEM. Once the water has spread over several depressions and reached point 5, there is a noticeable cumulative effect; the water levels rise significantly only after 35 h. For this test, therefore, the topography has a greater impact on the results than the physical complexity of the model.

RFSM-EDA is also used with mesh C, which matches the test specification with 10 000 IZs. As would be expected, the results have a close match to the other models. At point 4 they remain with 6 mm of JFLOW, and at point 5 the results lie in the middle of all the others, and are closest to JFLOW. Although not a model validation, this demonstrates that RFSM-EDA behaves as ex-pected when used with the same computational resolution as the other models.

The mesh A results show a significant improvement over the older dynamic RFSM, which reaches a peak level approximately 10 cm lower than the other models at point 4. At point 5 the dynamic RFSM's levels rise much too fast and finish ~4 cm higher than with InfoWorks and Tuflow.

The RFSM-EDA simulations using meshes A and B were computationally fast, with equal runtimes of ~0·9 s. A large proportion of this time was spent communicating with the SQL database that holds the data, and therefore increasing or decreas-ing the alpha value had little or no effect on simulation runtimes, and the increased topographic resolution of mesh 'B' did not slow the model relative to mesh 'A'. The depression shape of the IZs meant that there was a natural resistance to mass balance errors. The simulations were completed with alpha values of 1, with median time steps of ~62 s. No instabilities were found and the mass balance errors were 0%. The simulation with mesh C had only one sub-element cell in each IZ, so did not benefit from the IZ depression shape. However, it was also able to use an alpha value of 1 with only a 0·3% mass balance error.

Overall the results of test 2 show that RFSM-EDA can effectively predict propagation of flood waters over a complex domain. This is encouraging given that only 16 computational elements are used.

3.3 Test 4: Rate of propagation over extended floodplains

The speed of propagation of a flood wave is tested in test 4. A completely flat domain is used, with an inflow hydrograph applied at the centre of the left boundary, to produce a semi-circular flood wave. It is not possible to automatically generate the IZs as there is no topographic variation in the domain; a regular grid has therefore been used. The specified resolution is 5 m with approximately 80 000 elements. For this test, RFSM-EDA uses mesh A with 861 elements, 93 times fewer than the specification. There is no value in assessing results of mesh B or C due to the flat topography.

Figure 4 shows 15 cm depth contours at 1 h and 3 h after start of inundation. The coarse resolution means RFSM-EDA is not able to resolve the wetting front to the same level of detail as the other models. However, the speed of propagation is a significant improvement over the dynamic RFSM, which appears too slow and also appears to exhibit some oscillatory behaviour at the wetting front. InfoWorks and Tuflow predict the flow boundary in concentric circles, whereas RFSM-EDA exhibits a very slight preferential flow towards the diagonals, similar to Lisflood-ACC. This has been seen in several models that have the x and y flow directions decoupled (Neal *et al.*, 2011). For all tests completed by RFSM-EDA, this pattern has only been observed on perfectly flat topography when using a regular grid. It is therefore not expected in real topographic environments.

Figure 5 shows the level plot at point 2, 100 m from the inflow. As the RFSM-EDA's grid cells are large, the water reaches test point 2 marginally before the other models, but the form of the curve matches those of the other models well, with a peak level of 26·1 cm compared with 26·6 cm for Lisflood-ACC and 27·5 cm for Tuflow. RFSM-EDA's velocity profile has the correct shape, although the results are too low, with a peak velocity of 0·20 m/s compared with 0·23 m/s and 0·25 m/s for Lisflood-ACC and Tuflow, respectively. This may be due to the assumptions used in the area-averaging for the velocity calculations.

RFSM-EDA completed the test using an alpha value of 3, which produced a runtime of ~13 s, significantly faster than any other model (the fastest other model took nearly six times longer). This was achieved with zero mass balance errors.

3.4 Test 5: Valley flooding

Test 5 simulates a major flood inundation from a dam failure in a valley. The test domain has a constant downward slope with a hydrograph applied at the top of the valley. For mesh A, a regular square grid was adopted as few depressions could be found. The mesh had 530 elements, each 200 m square (except at the domain boundary), whereas the specified resolution was over 14 times this number of elements, with approximately 7600. For mesh C, 7643 IZs where used with one sub-element cell per IZ to match that of the other models.

Figures 6 and 7 respectively show the first and last test points in the domain. The IZs in mesh A generally have 16 sub-element cells in them. The test point will be at one of these cells, but normally at least one of the other 15 sub-element cells will have a lower level. This is why the levels for mesh A can be seen to start from a lower level than the other models. At point 1 the levels finish ~28 cm lower than Lisflood-ACC, and peak ~21 cm lower. It is clear that the Dynamic RFSM did not perform well for these tests, which is probably due to the use of flow limiters.

Mesh C shows that when running at the recommended resolution, RFSM-EDA produces results that are very similar to the other models. In fact, they are almost indistinguishable from those of
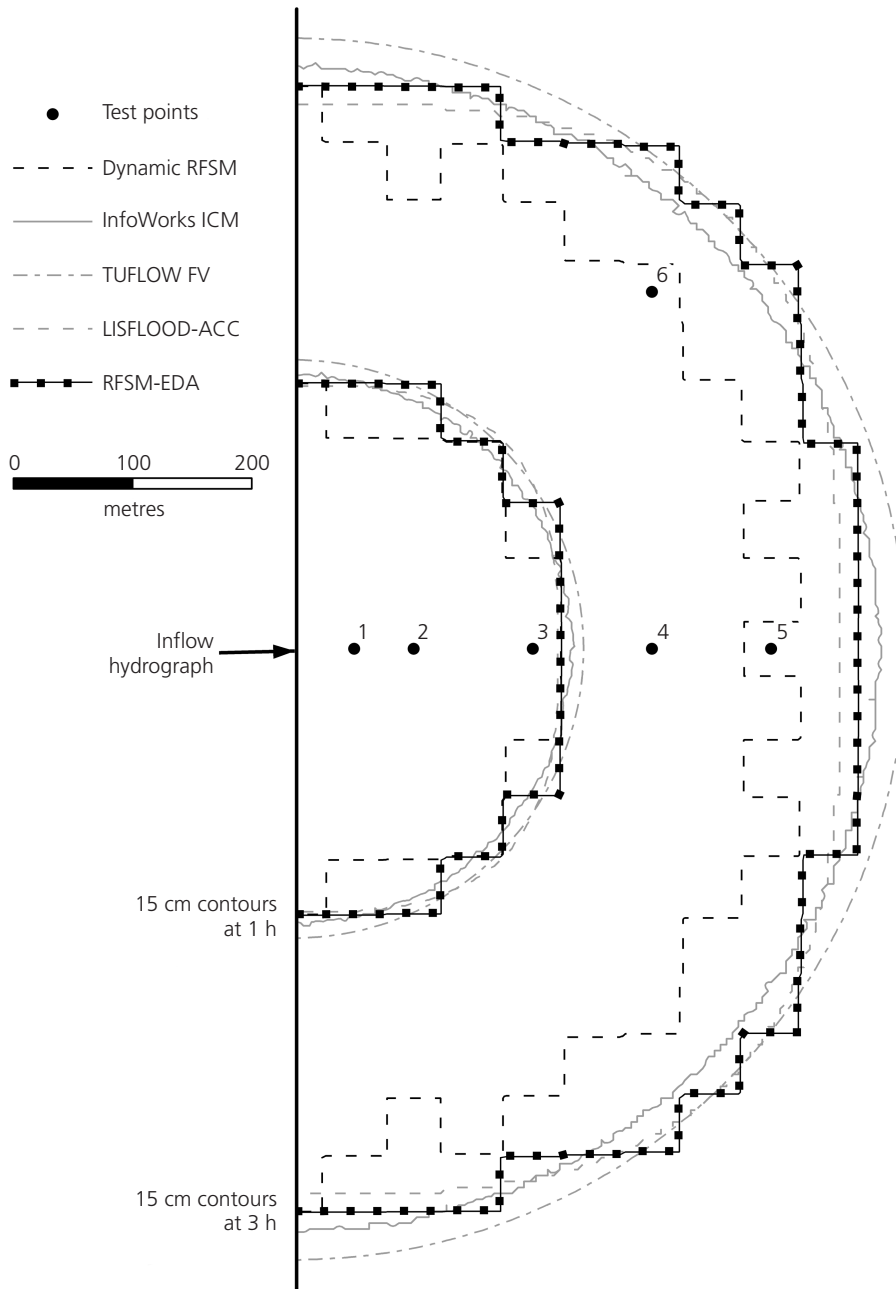
Figure 4. Depth contours (15 cm) at 1 h (inner concentric lines) and 3 h (outer concentric lines) for test 4

Lisflood-ACC. This is to be expected as when there is only one sub-element cell in the IZ the governing equations simplify to an equivalent of Bates *et al.* (2010). The differences seen between RFSM-EDA's results for mesh A and the other models are therefore primarily caused by the size of the IZs. Normally IZs have a natural resistance to over-rapid spreading of water, as each IZ must fill up a depression to the crest level before it can continue to flux. However, on test 5 there is an almost constant slope and very few depressions can be found. The IZs fill up from the lowest sub-element cell, and can immediately continue to flux, causing over-rapid down-slope wetting. This has a cumulative effect down the whole valley. At point 1 ($\sim$3·2 km from the inflow) the levels start to rise $\sim$7 min earlier than in the other models, but by point 5 ($\sim$15·7 km from the inflow) it is $\sim$50 min too early. The wetting front propagates at 7·1 km/h for RFSM-EDA, and at an average 5·2 km/h for the other models.

Water Management
Volume 165 Issue WM1

**A highly efficient 2D flood model with
sub-element topography**
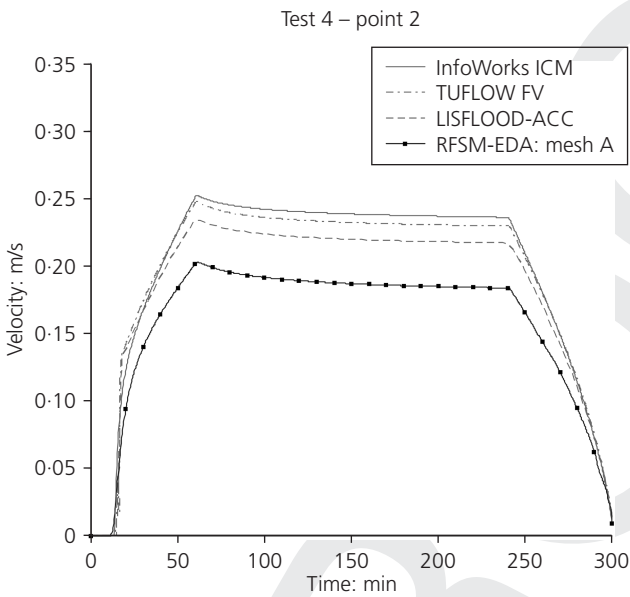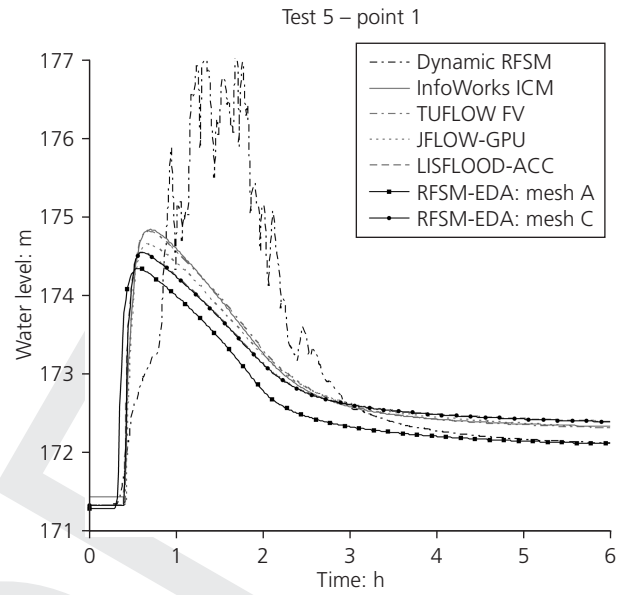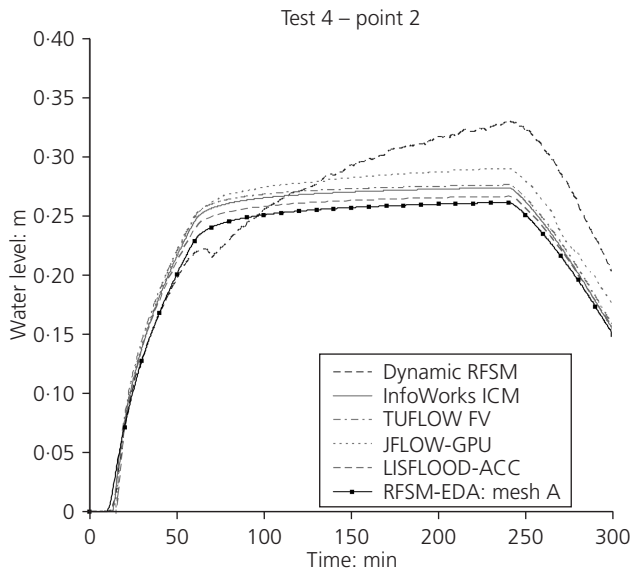Jamieson, Lhomme, Wright and Gouldby
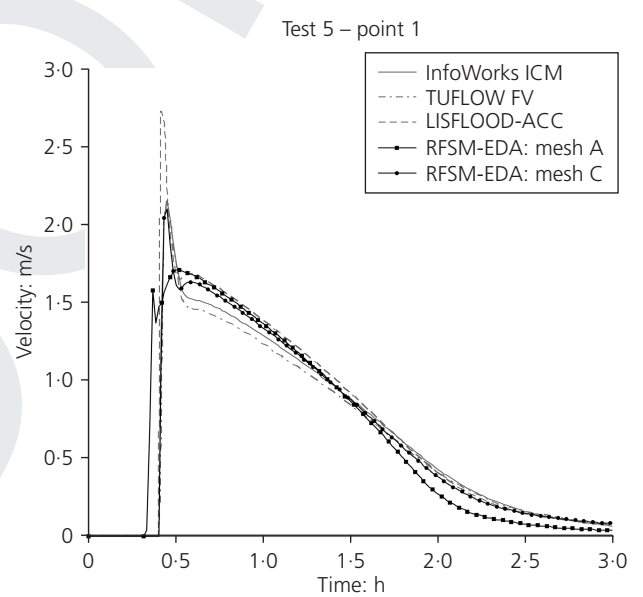
Figure 5. Levels and velocities for test 4 – point 2, 100 m from the inflow

Figure 6. Levels and velocities for test 5 – point 1, near the inflow source

The velocities predicted by RFSM-EDA (mesh A) match the other models well. At point 1 the velocities for RFSM-EDA remain within 0·15 m/s of the other models, except for a ~5 min window at 0·5 h where it peaks ~0·4–1 m/s lower. Adjusting for the time lag, at point 5 the velocities of RFSM-EDA remain within 0·1 m/s of the other models, except for a 15 min window when they are ~0·1–0·4 m/s lower.

RFSM-EDA (mesh A) was run with an alpha value of 2, which resulted in a final mass balance error of only 0·02%. It completes the simulation in ~14 s, which is significantly faster than all other models that undertook the test (ranging from 0·6 to

350 min). The mesh C model was also run with an alpha value of 2, and had zero final mass balance errors.

3.5 Test 8A: Rainfall and point source surface flow
This is a test of high-resolution modelling in an urban environment, initially from a global pluvial event, and subsequently from a surcharging culvert in the top right corner of the domain. The simulation is run long enough to allow the water to settle in the lower areas.

This test case has real topography and RFSM-EDA can therefore use its automatic mesh generation. The resulting IZs have quite
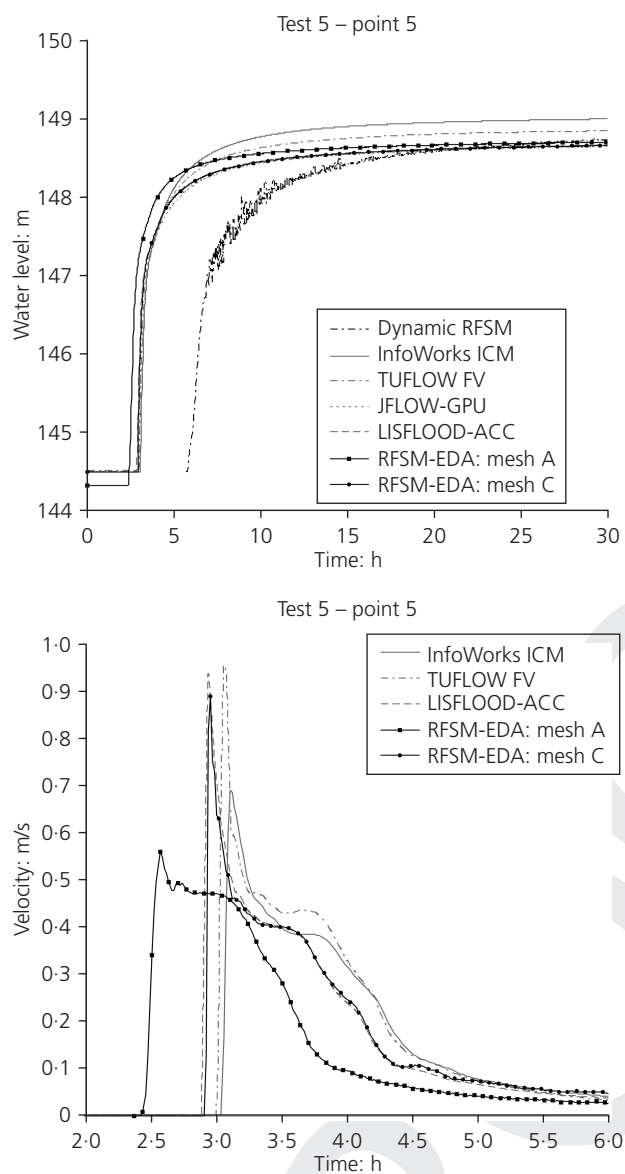
Water Management
Volume 165 Issue WM1

**A highly efficient 2D flood model with
sub-element topography**
Jamieson, Lhomme, Wright and Gouldby

Figure 7. Levels and velocities for test 5 – point 5, at the bottom of the valley

complex shapes and neighbour relations, as shown in Figure 8. Mesh A has 1786 IZs with the recommended topographic resolution of 2 m. This is ~54 times fewer than the specified 97 000 elements. Mesh B is also used, which has 2207 elements and a sub-element resolution of 0·5 m.

The results for RFSM-EDA are good considering that the scale of the test is far smaller than the model was designed for. Results for meshes A and B both have levels approximately 10 cm higher than the other models at point 7 for both the first and second peaks (Figure 9). For point 8 (Figure 10), mesh A results are ~8 cm higher at the first peak and 1–2 cm lower for the second peak, whereas mesh B results are 1–2 cm higher for both peaks. The final levels are similar for all models in point 7, but very

widely spread for point 8. This indicates that the different models have likely sampled or averaged the raw DTM in different ways. The dynamic RFSM performs poorly and does not match the shape of the curves as well as RFSM-EDA does. Although the timing of the velocities is good, the magnitudes are lower for both meshes; roughly half that of the other models, with mesh B tending to have greater velocities. The IZs have complex shapes which encompass the major flow routes on the roads (where the test points are located) as well as the areas surrounding the roads. It is likely therefore that the lower velocities are a result of the velocity area-averaging over the large IZs.

While the local response of RFSM-EDA may differ in a few places from the other models, the overall model response is similar, and is illustrated by comparing the depth contours over the domain (Figure 11); note that to avoid complication, only the results of RFSM-EDA (mesh A) and Tuflow FV are shown in Figure 11. RFSM-EDA appears to match Tuflow very well for depths of 20 cm, but the lower depths of 5 cm are not very well depicted in certain parts of the domain, particularly the sloped areas to the east. This is investigated further by calculating the F-statistic, which measures the predictive accuracy of the inundated area (Horritt and Bates, 2001) relative to the Tuflow results. Mesh A has an F value of 54% for depths greater than 5 cm. When the depth threshold is increased to 20 cm, mesh A has an F value of 69%. For mesh B the predictions are 53% and 71%, respectively. Clearly RFSM-EDA has some difficulties simulating the shallow flow paths, but when greater depths are considered it performs much better. There is no major difference in the results of mesh A and B.

RFSM-EDA is run with an alpha parameter of 4 for these tests. For mesh A this gives a runtime of 2·90 min, much faster than any other model, and with a mass balance error of only 0·06%. For mesh B it runs in 4·32 min with a mass balance error of 0·83%. The longer runtime for mesh B is partially because it has ~24% more IZs, but it is also due to the finer sub-element resolution. On average an IZ in mesh B has ~27 sub-element cells in each interface, whereas mesh A has only ~6. This means that simulations using mesh B have a lot more calculations to undertake for the interface fluxes than simulations using mesh A.

3.6 Computational efficiency
Unlike most similar models, the data needed to run RFSM-EDA is stored in an SQL database. This allows for efficient modularisation within probabilistic modelling frameworks like MDSF2, but it can slow down the simulation through read and write access to the SQL server. Whilst this is not generally an issue unless a high frequency of intermediate results are required, it can dominate the performance in very short tests: for example, in test 2A one-fifth of the simulation time is spent in initialisation.

The simulation times for all models/tests are given in Table 3. It is important to note that these results may not present a fair comparison, as computers with varying specifications have been
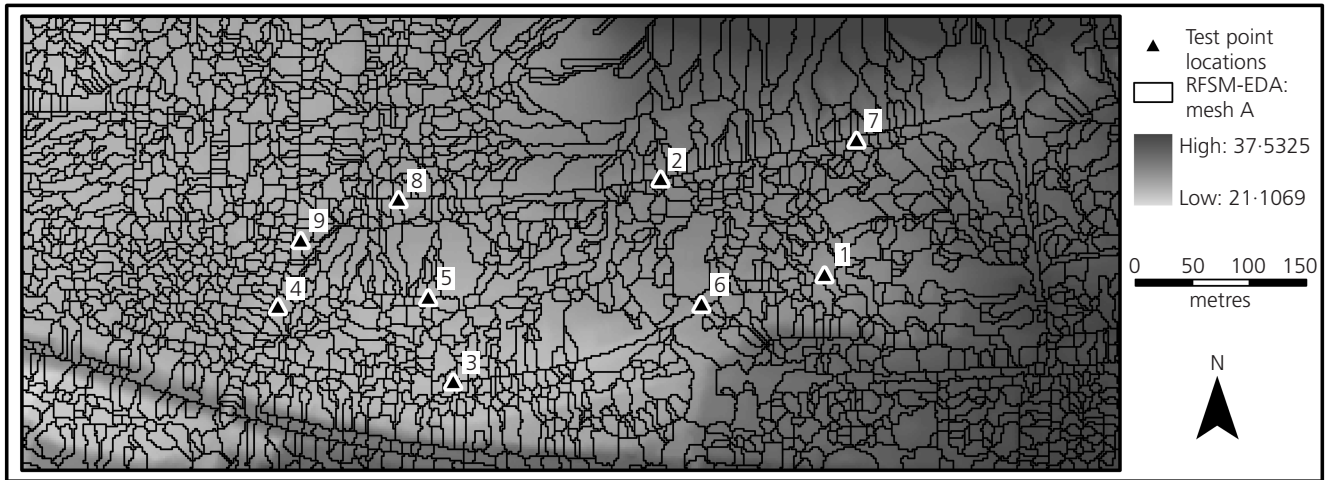
Figure 8. Impact zones in RFSM-EDA mesh A for test 8A, with DEM
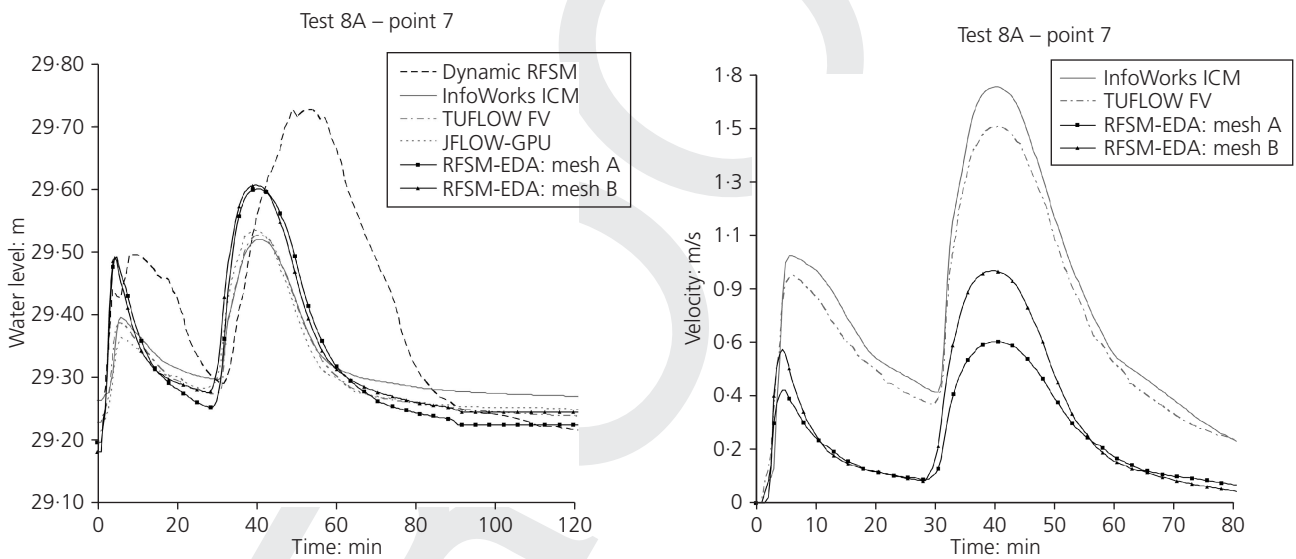

Figure 9. Levels and velocities for test 8a – point 7

used and some of the models also used parallel processing (e.g. Tuflow-FV, InfoWorks-ICM and JFLOW-GPU).

Table 3 clearly shows that RFSM-EDA is fast; the fastest in every test attempted. This has been achieved without the benefit of parallelisation. It performs well in these tests primarily because it was possible to maximise the benefit of the sub-element representation while undertaking the computations on a coarse grid. At larger spatial scales, for which the model has been developed, further benefits are likely to be realised.

It is also expected that using a single flux calculation (based on total interface properties as opposed to the compound section currently used) would significantly improve simulation runtimes.

4. Discussion

RFSM-EDA was designed to be used on large (city/regional) scales with variable (i.e. real) topography. The EA's benchmark tests are small scale and a number have artificially smooth topography. Despite this, the RFSM-EDA has demonstrated an ability to generate results that are in line with those of models that comprise a more complex representation of the physical processes and thus take a longer computational time. Moreover, RFSM-EDA can incorporate even finer-scale topography with
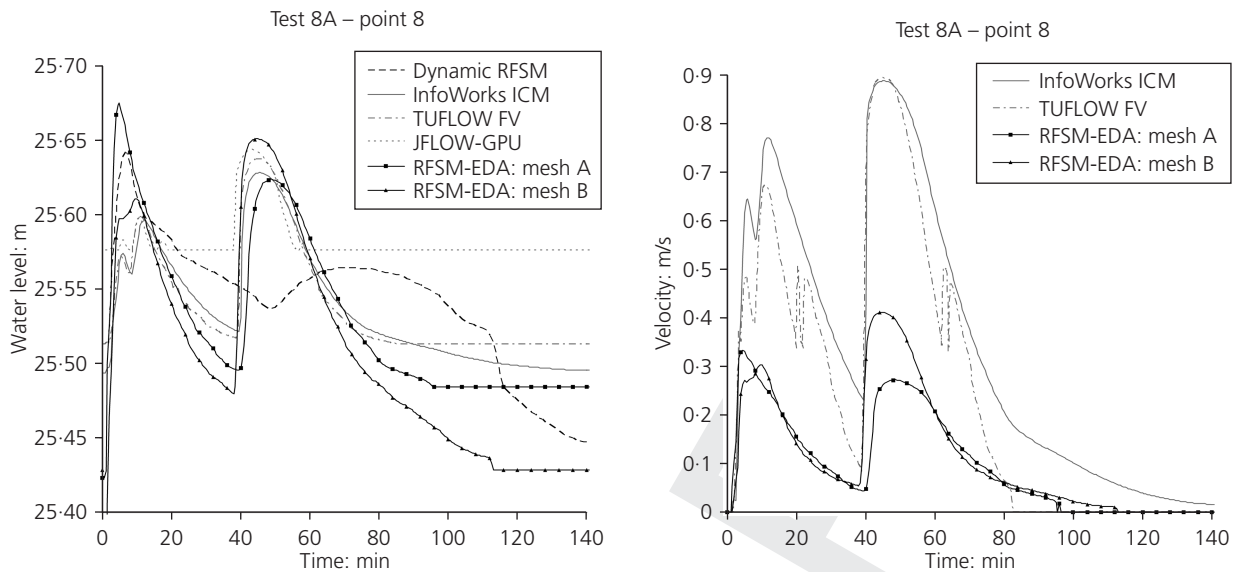
Figure 10. Levels and velocities for test 8a – point 8
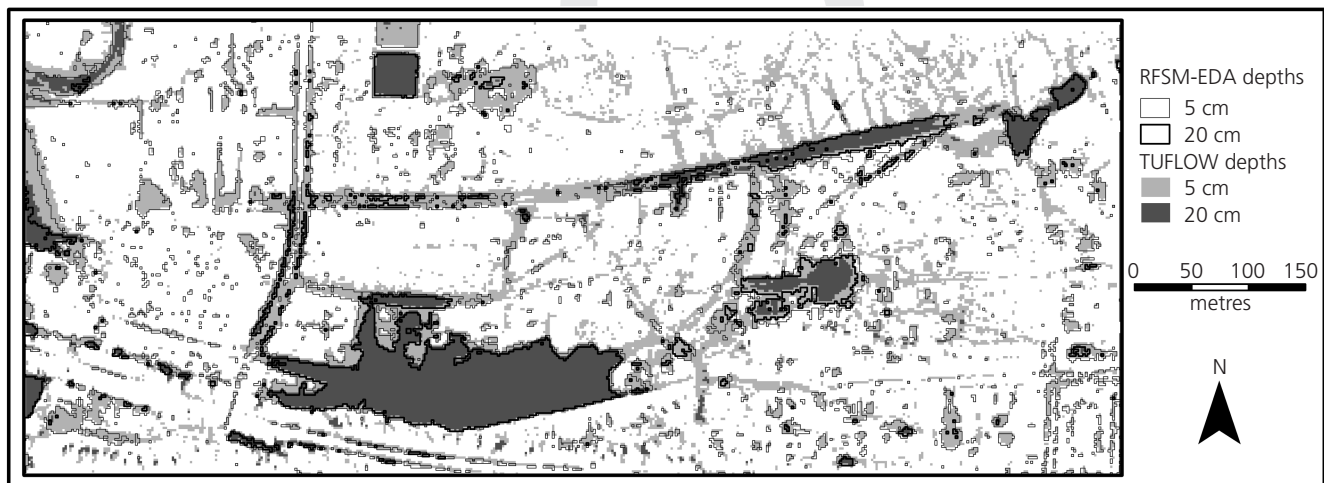

Figure 11. Depth contours for RFSM-EDA and Tuflow FV for test 8A

minimal impact on runtimes. This reduces the need of the modeller to introduce additional uncertainties to the modelling process by averaging or re-sampling the DEM. Given that much of the flood modelling undertaken in the UK is at larger spatial scales and often of a probabilistic nature, it may be appropriate to consider the introduction of additional tests that are able to appropriately verify models that are developed for this purpose.

The schematisation of RFSM-EDA means that water fills from the lowest point in an impact zone. On the relatively rare occasion that natural floodplain depressions do not exist, such as in test 5, water leaves an impact zone immediately upon wetting. This results in an overestimation of propagation speed by 36%.

For large-scale probabilistic modelling this source of error is unlikely to be significant, and the results presented herein show that peak levels and flows are predicted reasonably accurately (see Figures 5 and 6). In other situations where RFSM-EDA results differ more markedly from those of the other models presented here, it is worth considering that the EA benchmarking report includes many more model results (Wright *et al.*, 2012), and the peak flood levels of RFSM-EDA are within the spread of these results.

The sub-element representation in RFSM-EDA offers an effective approach for reducing runtime while preserving or, in some cases, increasing topographic accuracy. The results using the

Water Management
Volume 165 Issue WM1

**A highly efficient 2D flood model with
sub-element topography**
Jamieson, Lhomme, Wright and Gouldby

Model	Computation time in minutes for each test			
	2	4	5	8A
RFSM-EDA (mesh A)	**0·015**	**0·21**	**0·23**	**2·9**
Dynamic RFSM	0·19	5·8	9·8	23·3
Tuflow FV	2·64	24·5	2·9	72·6
InfoWorks ICM[a]	0·73	6·5	0·7	27·1
JFLOW-GPU	1·83	2·3	10·2	16·2
Lisflood-ACC[b]	n/a	1·97	0·68	n/a
Fastest other[c]	0·4	1·27	0·6	4
Slowest other[c]	130	282·8	350	307·8

[a] The runtimes are taken from InfoWorks RS, but the results in this paper are from InfoWorks ICM; little difference is expected.
[b] Lisflood-ACC runtimes appear in Neal *et al.* (2011).
[c] Fastest and slowest models other than those shown in this paper, but appearing in Wright *et al.* (2012).

Table 3. Simulation runtimes for different models, fastest in bold type

recommended DEM resolution matched the other models well. In some cases, such as test 2A, using an even higher DEM resolution produced a step change in model response, which implies that the topography has a greater effect on simulation results than process representation. Additionally, because the mesh is automatically aligned to topographic features such as embankments and dykes, it will always respect the effect they have on propagation directions, regardless of grid scale.

The adaptive time step used by RFSM-EDA has shown to be effective for all tests. Unlike Lisflood-ACC, which generally needs alpha values significantly below unity (Neal *et al.*, 2011), RFSM-EDA is stable with a value of 1 or significantly above. The fact that the alpha value could be as large as 4 in test 8A implies that the CFL condition used (Equation 7) may be conservative for this algorithm. It is likely that this is due to the inclusion of the velocity vector in the CFL condition, which is not included in the original model of Bates *et al.* (2010). Although several other diffusive models use velocity in their stability condition, such as Bradbrook *et al.* (2004), an alternative formulation that excludes velocity may be more appropriate for RFSM-EDA.

Although the results have already been shown to be good for these small tests, there is potential for further improvements. In test 5 the propagation speeds are too fast down the valley, which is primarily caused by the large computational elements. Future work should aim to find an approach to limit the propagation speeds for large computational elements. Using a single flux calculation at the interface, rather than a summation of panel fluxes, has the potential to make RFSM-EDA considerably faster still, although the impact on simulation accuracy will require

verification. Some investigations may be necessary to see whether predictions of low-depth flow paths can be improved, as in test 8A, but these shallow flow paths are less important for probabilistic risk calculations than greater depths.

The RFSM-EDA has been developed specifically for use at larger spatial scales and within the context of probabilistic simulations. The model provides a step-change in accuracy over previous versions, the dynamic RFSM and the direct RFSM (which is currently used within the Environment Agency's NaFRA and MDSF2 systems). This significant improvement comes with the price of additional computational expense over the direct RFSM. The computational expense is however, a fraction of that associated with alternative models that solve the full SWE on conventional grid systems. The model therefore provides a good compromise between practical computational times, while providing robust flood simulations.

5. Conclusions
RFSM-EDA has been applied to six of the EA's hydraulic benchmarking tests, four of which are shown in this paper. The model was designed to be used on larger domains of naturally varying topography, but nonetheless has performed well given the small-scale nature of the tests. The peak levels predicted by RFSM-EDA differed by less than ± 10 cm from the other models in all cases except for test 5, where they were within ± 50 cm. This is a mesh effect rather than a numerical inaccuracy, as when using an equivalent mesh resolution the results were visually identical to those of Lisflood-ACC. The velocity predictions had a similar form to the other models, though they tended to be 20–60% lower. This is primarily because an impact zone average velocity is used; using a maximum velocity would be more

Water Management
Volume 165 Issue WM1

A highly efficient 2D flood model with
sub-element topography
Jamieson, Lhomme, Wright and Gouldby

conservative. RFSM-EDA clearly offers a step change in accuracy over the direct RFSM and dynamic RFSM, while comparing favourably with industry standard codes. As RFSM-EDA can increase topographic resolution without needing to increase the number of computational elements, it is able to improve simulation accuracy further with minimal change in computational burden.

RFSM-EDA was the fastest of all models by a considerable margin on all of the tests (less than a tenth of the average runtime of the models shown here, and between 4% and 73%, depending on the test, of the runtime of the otherwise fastest model). It has the potential to be even faster if simpler flux calculations and parallelisation are implemented. Additional testing on very large regional domains is underway, and it is likely that the benefits of the scheme will become even more apparent as the trade-off between simulation time and grid resolution becomes more severe for conventional models.

RFSM-EDA has completed a selection of the EA benchmarking tests with fast runtimes and results accurate enough for broad-scale flood risk assessments. The tests present a proof of concept, and demonstrate that the model has the potential to be an effective tool for large-scale and probabilistic inundation modelling.

Acknowledgements

REFERENCES
Bates P and De Roo A (2000) A simple raster-based model for flood inundation simulation. *Journal of Hydrology* **236(??)**: 54–77.

Bates P, Horritt M and Fewtrell T (2010) A simple inertial formulation of the shallow water equations for efficient two-dimensional flood inundation modelling. *Journal of Hydrology* **387(??)**: 33–45.

Beven K and Binley A (1992) The future of distributed models – model calibration and uncertainty prediction. *Hydrological Processes* **6(??)**: 279–298.

Bradbrook K, Lane S, Waller S and Bates P (2004) Two dimensional diffusion wave modelling of flood inundation using a simplified channel representation. *International Journal of River Basin Management* **2(??)**: 211–223.

Casulli V and Stelling G (2011) Semi-implicit subgrid modelling of three-dimensional free-surface flows. *International Journal for Numerical Methods in Fluids* **67(??)**: 441–449.

Chen A, Djordjevic S, Leandro J, Evans B and Savic D (2008) Simulation of the building blockage effect in urban flood modelling. *11th International Conference on Urban Drainage, Edinburgh, UK*, pp. ■■■–■■■.

Environment Agency (2009) *Flooding in England: A National Assessment of Flood Risk*. Environment Agency, Bristol, UK.

Environment Agency (2010) *Benchmarking of 2D Hydraulic Modelling Packages*. SC080035/SR2. Environment Agency, Bristol, UK.

Environment Agency (2011) *MDSF2 Technical Report, Science Report SC050051/SR4*. Environment Agency, Bristol, UK.

Estrela T and Quintas L (1994) Use of a GIS in the modelling of flows on floodplains. In *2nd International Conference on River Flood Hydraulics, York, UK* (White W and Watts J (eds)).

EC (European Parliament and Council of the European Union) (2007) Directive 2007/60/EC of the European Parliament and of the Council of 23 October 2007, On the assessment and management of flood risks. *Official Journal of the European Union*, L288/27.

Evans E, Hall J, Penning-Roswell E *et al.* (2006) Future flood risk management in the UK. *Proceedings of the Institution of Civil Engineers – Water Management* **159(1)**: 53–61.

Fewtrell TJ, Bates PD, Horritt M and Hunter NM (2008) Evaluating the effect of scale in flood inundation modelling in urban environments. *Hydrological Processes* **22(??)**: 5107–5118.

Fewtrell T, Duncan A, Sampson C, Neal J and Bates P (2011) Benchmarking urban flood models of varying complexity and scale using high resolution terrestrial LiDAR data. *Physics and Chemistry of the Earth* **36(??)**: 281–291.

Gouldby B, Sayers P, Mulet-Marti J, Hassan M and Benwell D (2008a) A methodology for regional-scale flood risk assessment. *Proceedings of the Institution of Civil Engineers-Water Management* **161(??)**: 169–182.

Gouldby B, Sayers P and Tarrant O (2008b) Application of a flood risk model to the Thames Estuary for economic benefit assessment. In *Risk Analysis VI:Simulation and Hazard Mitigation* (Brebbia CA and Beriatos E (eds)). WIT Press, Caephalonia, pp. 11–19.

Guinot V and Soares-Frazao S (2006) Flux and source term discretization in two-dimensional shallow water models with porosity on unstructured grids. *International Journal for Numerical Methods in Fluids* **50(??)**: 309–345.

Hall JW, Dawson RJ, Sayers PB *et al.* (2003) A methodology for national-scale flood risk assessment. *Proceedings of the Institution of Civi Engineers – Maritime Engineering* **156(3)**: 235–247.

Hartnack J, Enggrob H and Rungo M (2009) 2D overland flow modelling using fine scale DEM with manageable runtimes. In *Flood Risk Management: Research and Practice* (Samuels P (ed)). Taylor and Francis, London.

Horritt M and Bates P (2001) Effects of spatial resolution on a raster based model of flood flow. *Journal of Hydrology* **253(??)**: 239–249.

7

8

9

10

11

12

HR Wallingford (2006) *Rapid Flood Spreading Methodology (RFSM)*. Thames Estuary 2100 Report DT4. Environment Agency, Bristol, UK.

Hunter NM, Horritt MS, Bates PD, Wilson MD and Werner MGF (2005) An adaptive time step solution for raster-based storage cell modelling of floodplain inundation. *Advances in Water Resources* **28(??)**: 975–991.

Hunter NM, Bates PD, Neelz S *et al.* (2008) Benchmarking 2D hydraulic models for urban flooding. *Proceedings of the Institution of Civil Engineers – Water Management* **161(??)**: 13–30.

Innovyze (2011) *Infoworks 11·5 RS Help*. Innovyze, Broomfield, CO, USA.

Lamb R, Crossley M and Waller S (2009) A fast two-dimensional floodplain inundation model. *Proceedings of the Institution of Civil Engineers – Water Management* **162(??)**: 363–370.

Lhomme J, Sayers P, Gouldby B, Samuels P and Wills M (2009) Recent development and application of a rapid flood spreading method. In *Flood Risk Management: Research and Practice* (Samuels P (ed.)) Taylor and Francis, London, UK, pp.15–24.

Lhomme J, Gutierrez-Andres J, Weisgerber A *et al.* (2010) Testing a new two-dimensional flood modelling system: analytical tests and application to a flood event. *Journal of Flood Risk Management* **3(??)**: 33–51.

Lhomme J, Jamieson S and Gouldby B (2012) A fast 2D diffusive wave model with sub-element resolution for large scale flood mapping. In preparation.

Mark O, Weesakul S, Apirumanekul C, Aroonnet S and Djordjevic S (2004) Potential and limitations of 1D modelling of urban flooding. *Journal of Hydrology* **299(??)**: 284–299.

McMillan H and Brasington J (2007) Reduced complexity strategies for modelling urban floodplain inundation. *Geomorphology* **80(3–4)**: 226–243.

National Audit Office (2011) *Flood Risk Management in England*. The Stationary Office, London, UK.

Neal J, Villanueva I, Wright N *et al.* (2011) How much physical complexity is needed to model flood inundation? *Hydrological Processes* **26**, http://dx.doi.org/10.1002/hyp.8339.

Romanowicz R and Beven K (2003) Estimation of flood inundation probabilities as conditioned on event inundation maps. *Water Resources Research* **39(3)**: http://dx.doi.org/1029/2001WR001056.

Romanowicz R, Beven KJ and Tawn J (1996) Bayesian calibration of flood inundation Models. In *Floodplain Processes* (Anderson MG, Walling DE and Bates PD (eds)). Wiley, Chichester, UK, pp. ■■■–■■■.

Wright N, Neelz S and Pender G (2012) EA 2D Benchmarking Study. *Proceedings of the Institution of Civil Engineers – Water Management*, this issue.

Yu D and Lane S (2006a) Urban fluvial flood modelling using a two-dimensional diffusion-wave treatment, part 1: mesh resolution effects. *Hydrological Processes* **20(??)**: 1541–1565.

Yu D and Lane S (2006b) Urban fluvial flood modelling using a two-dimensional diffusion-wave treatment, part 2: development of a sub-grid-scale treatment. *Hydrological Processes* **20(??)**: 1567–1583.

Yu D and Lane S (2011) Interactions between subgrid-scale resolution, feature representation and grid-scale resolution in flood inundation modelling. *Hydrological Processes* **25(??)**: 36–53.

Zanobetti D, Longeré H, Preissmann A and Cunge J (1970) Mekong Delta mathematical model program construction. *Journal of the Waterways and Harbors Division* **96(??)**: 181–199.

Zhang WH and Cundy TW (1989) Modelling of two-dimensional overland-flow. *Water Resources Research* **25(??)**: 2019–2035.

1: Goulby – is Spain the appropriate location for the second affiliation?
2: Is the use of this "alternative" Greek sigma rather than the usual σ intentional and for a purpose?
3: Woodward et al. 2011 is not listed in References.
4: DEM has not been "defined" – spell out at first use.
5: Head 3 was followed by 3.1.1. A heading 3.1 is required between them. The alternative is to re-number all the sub-head in Section 3.
6: PRODUCTION: this paper is in this issue; see list
7: Where (??) is appended to a volume number, please supply the issue number if there is one.
8: Beven K and Binley A (1992) – This reference does not appear to be cited in the text.
9: Chen et al. 2008 – page numbers in Proceedings? Who si the sponsor/publisher?
10: Estrela T and Quintas L (1994) – Name and location of publisher of Proceedings?
11: Fewtrell TJ, Bates PD, Horritt M and Hunter NM (2008) – This reference does not appear to be cited in the text.
12: Fewtrell T, Duncan A, Sampson C, Neal J and Bates P (2011) – This reference does not appear to be cited in the text.
13: Lhomme J, Jamieson S and Gouldby B (2012) – Include only if "in press" by proof stage. Otherwise delete from list and cite in text as "unpublished".
14: Neal J, Villanueva I, Wright N *et al.* (2011) – include publication details as well as DOI.

15: Romanowicz R and Beven K (2003)– include publication details as well as DOI
16: Romanowicz R, Beven KJ and Tawn J (1996) – page numbers?
17: PRODUCTION: Add details when the issue is paginated.